



## White matter microstructure is associated with cognitive control in children<sup>☆</sup>



Laura Chaddock-Heyman<sup>a,\*</sup>, Kirk I. Erickson<sup>b</sup>, Michelle W. Voss<sup>c</sup>, John P. Powers<sup>d</sup>, Anya M. Knecht<sup>a</sup>, Matthew B. Pontifex<sup>e</sup>, Eric S. Drollette<sup>f</sup>, R. Davis Moore<sup>f</sup>, Lauren B. Raine<sup>f</sup>, Mark R. Scudder<sup>f</sup>, Charles H. Hillman<sup>f</sup>, Arthur F. Kramer<sup>a</sup>

<sup>a</sup> Department of Psychology & Beckman Institute, University of Illinois at Urbana-Champaign, 405 North Mathews Avenue, Urbana, IL 61801, United States

<sup>b</sup> Department of Psychology, University of Pittsburgh, Sennott Square, Third Floor, 210 South Bouquet Street, Pittsburgh, PA 15260, United States

<sup>c</sup> Department of Psychology, The University of Iowa, E11 Seashore Hall, Iowa City, IA 52242, United States

<sup>d</sup> Department of Neurology, The University of Pennsylvania, 3400 Spruce Street, 3 West Gates, Philadelphia, PA 19104, United States

<sup>e</sup> Department of Kinesiology, Michigan State University, 308 W. Circle Drive, East Lansing, MI 48824, United States

<sup>f</sup> Department of Kinesiology & Community Health, University of Illinois at Urbana-Champaign, 906 South Goodwin Avenue, Urbana, IL 61801, United States

### ARTICLE INFO

#### Article history:

Received 30 October 2012

Accepted 13 May 2013

Available online xxx

#### Keywords:

Child

Cognition

Diffusion tensor imaging

Flanker

MRI

### ABSTRACT

Cognitive control, which involves the ability to pay attention and suppress interference, is important for learning and achievement during childhood. The white matter tracts related to control during childhood are not well known. We examined the relationship between white matter microstructure and cognitive control in 61 children aged 7–9 years using diffusion tensor imaging (DTI). This technique enables an *in vivo* characterization of microstructural properties of white matter based on properties of diffusion. Such properties include fractional anisotropy, mean diffusivity, axial diffusivity, and radial diffusivity, measures thought to reflect specific biological properties of white matter integrity. Our results suggest that children with higher estimates of white matter integrity in the corona radiata, superior longitudinal fasciculus, posterior thalamic radiation, and cerebral peduncle were more accurate during incongruent (>><<), <<>> and neutral (-->-, --<--) trials of a task of cognitive control. Importantly, less interference during the task (i.e., incongruent and neutral difference scores) was associated with greater white matter microstructure in the posterior thalamic radiation and cerebral peduncle. Fiber tracts in a frontal–parietal–striatal–motor circuit seem to play a role in cognitive control in children.

Published by Elsevier B.V.

### 1. Introduction

Recent advances in neuroimaging enable us to study how brain regions are integrated into networks to support cognitive function. Here we apply diffusion tensor imaging (DTI) to a child population to investigate how the microstructural organization of white matter tracts is related to cognitive control. Individual differences in cognition during childhood have been associated with variations in brain structure and brain function, including gray matter volumes and functional brain networks (Bunge & Crone, 2009; Shaw et al., 2006). Clearly, maturation of white matter tracts also plays a critical role in the development of cognitive functions. Yet, the white

matter tracts most important to cognitive control during childhood are not well known. The present study examined the relationship between white matter microstructure and performance on a task of cognitive control in 7–9-year-old children. Cognitive control (also known as ‘executive control’) refers to the ability to guide behavior toward specific goals, formulate decisions, and control action (Bunge & Crone, 2009), processes that involve the ability to selectively attend to relevant information and filter distracting information.

DTI enables an *in vivo* characterization of microstructural properties of white matter based on properties of diffusion, and the information is represented mathematically in a diffusion ellipsoid (Johansen-Berg & Behrens, 2009; Jones, 2011; Mori, 2007; Rykhlevskaia, Gratton, & Fabiani, 2008). Different DTI measures are hypothesized to reflect specific biological properties of white matter microstructure. High levels of fractional anisotropy (FA) (i.e., increased directionality of diffusion) are said to occur in tightly bundled, structurally compact fibers with high integrity (Basser, 1995; Beaulieu, 2002; Rykhlevskaia et al., 2008; Sen & Basser, 2005). One component of FA is mean diffusivity (MD), calculated as the mean of all three axes of the diffusion ellipsoid, and considered an

<sup>☆</sup> Funding was provided by a grant from the National Institute of Child Health and Human Development (392 NIH 1 R01 HD069381).

\* Corresponding author at: Department of Psychology, The Beckman Institute for Advanced Science and Technology, University of Illinois at Urbana-Champaign, 405 North Mathews Avenue, Urbana, IL 61801, United States. Tel.: +1 610 209 6836; fax: +1 217 333 2922.

E-mail address: [lchaddo2@illinois.edu](mailto:lchaddo2@illinois.edu) (L. Chaddock-Heyman).

estimation of membrane density (Schmithorst & Yuan, 2010). Diffusion along the major axis/eigenvector of the ellipsoid is termed axial diffusivity (AD), which may reflect the pathology of axonal fibers including axonal diameter, loss or damage (Budde et al., 2007; Song et al., 2003). Radial diffusivity (RD) is the average of the second and third minor axes (Basser, 1995; Pierpaoli & Basser, 1996; Pierpaoli, Jezzard, Basser, Barnett, & Di Chiro, 1996; Song et al., 2002) and is considered to reflect insulated, myelinated tracts (Budde et al., 2007; Nair et al., 2005; Rykhlevskaia et al., 2008; Song et al., 2002; Song et al., 2003; Song et al., 2005). Investigating patterns of diffusivity across the brain permits the characterization of microstructural white matter properties that are important for paying attention and inhibiting distractions, skills important in and out of the school environment (Bull & Scerif, 2001; DeStefano & LeFevre, 2004; St. Clair-Thompson & Gathercole, 2006).

A number of studies have reported a positive relationship between various cognitive abilities (e.g., reading, IQ, information processing, visual-spatial working memory, attention, interference suppression, response inhibition) and different measures of white matter microstructure across a variety of fiber tracts throughout the lifespan (see Madden et al., 2012; Schmithorst & Yuan, 2010 for reviews of literature on young and older populations). Most research has focused on the relationship between white matter structure and cognition in late life (Madden et al., 2012). Only a few investigations have examined the relationship between estimates of white matter integrity and cognitive control in healthy, typically developing children. Cognitive control is supported by a network of frontal, parietal, striatal and motor regions (Banich et al., 2000). For example, in terms of attentional control and interference control, one voxel-wise DTI study examined flanker task performance consistency (i.e., trial-to-trial intraindividual variability of reaction time [RT]) in 8–19-year-olds and found that less response time variability was associated with better estimates of white matter integrity (e.g., FA) in frontal (e.g., corpus callosum), parietal, and corticospinal tracts, independent of age (Tamnes, Fjell, Westlye, Ostby, & Walhovd, 2012). However, no significant associations between diffusion measures (FA, MD, AD, RD) and mean RT were reported (Tamnes et al., 2012). Here, we limit our age range to 7–9-year-old children to focus on the tracts important during this period of preadolescent childhood. In addition, we focus on the relationship between white matter microstructure and performance in terms of both accuracy and RT, because individual differences in accuracy may be as or even more informative in a childhood population (Davidson, Amso, Anderson, & Diamond, 2006; Tamnes et al., 2012).

In terms of inhibitory control, one study used tractography to examine the relationship between connectivity in specific white matter tracts between the frontal cortex and striatum and performance on a Go/NoGo task in a sample of 7–31-year-olds (Liston et al., 2006). The researchers reported that more restricted radial diffusivity (RD) in frontostriatal fibers, but not corticospinal tracts, predicted individual differences in cognitive control, independent of age. Additionally, in a sample of children aged 7–13, faster response inhibition during a stop signal task was associated with higher FA and lower perpendicular diffusivity in fiber tracts within frontal and motor cortex regions (i.e., inferior frontal gyrus, supplementary motor cortex), independent of age (Madsen et al., 2010). Clearly, additional research is needed to understand how white matter structure relates to cognitive control during childhood.

We extend this literature in several important ways in our current study. We predicted that white matter microstructure would be associated with cognitive control in children. We made *a priori* hypotheses about specific white matter fibers involved in cognitive control given that certain tracts have been found to relate to cognitive and motor abilities across the lifespan (Liston et al., 2006; Madden et al., 2012; Schmithorst & Yuan, 2010; Tamnes

et al., 2012). Firstly, we investigated the corpus callosum, a tract that connects the left and right cerebral hemispheres and facilitates interhemispheric communication. Secondly, we made a region of interest (ROI) of the corona radiata, a tract that carries ascending and descending information from the cerebral cortex and has been found to relate to different elements of cognitive control across the lifespan, including attention, working memory, visual-spatial memory, and processing speed (Bendlin et al., 2010; Niogi, Mukherjee, Ghajar, & McCandliss, 2010; Olesen, Nagy, Westerberg, & Klingberg, 2003). Thirdly, we examined the superior longitudinal fasciculus, a tract providing the bidirectional information transfer between the frontal and parietal cortex (Petrides & Pandya, 1984; Schmahmann & Pandya, 2006) which plays a role in working memory in children (Nagy, Westerberg, & Klingberg, 2004) and older adults (Burzynska et al., 2011). Fourthly, we created an ROI of the posterior thalamic radiation, nerve fibers connecting thalamus with the cerebral cortex by way of internal capsule (which separates the caudate nucleus and the thalamus from the lenticular nucleus). Fifthly, we investigated the cerebral peduncle, part of the brainstem, which includes corticospinal tract, corticobulbar tract, and other nerve tracts conveying motor information to and from the brain to the rest of the body. In general, we predicted that higher FA and lower overall diffusivity of these tracts would relate to higher performance, and less interference, during a task measuring cognitive control in 7–9-year-olds.

## 2. Method

### 2.1. Participants

Sixty-one prepubescent (Taylor et al., 2001) children (33 girls, 28 boys), ages 7–9 years ( $M = 8.7$  years,  $SD = 0.6$ ), from East-Central Illinois were included in the analysis. To be eligible for the study, children had to have a Kaufman Brief Intelligence Test (KBIT) score greater than 85 (Kaufman & Kaufman, 1990) and qualify as prepubescent (Tanner puberty score  $\leq 2$ ; Taylor et al., 2001). Children were also screened for the presence of attentional disorders using the Attention Deficit Hyperactivity Disorder (ADHD) Rating Scale IV (DuPaul, Power, Anastopoulos, & Reid, 1998), and were excluded if they scored above the 85th percentile. Eligible children were further required to (1) report an absence of school-related learning disabilities (i.e., individual education plan related to learning), adverse health conditions, physical incapacities, or neurological disorders, (2) report no use of medications that influence central nervous system function, (3) demonstrate right handedness (as measured by the Edinburgh Handedness Questionnaire; Oldfield, 1971), (4) complete a mock MRI session successfully to screen for claustrophobia in an MRI machine, and (5) sign an informed consent approved by the University of Illinois at Urbana-Champaign. A legal guardian also provided written informed consent in accordance with the Institutional Review Board of the University of Illinois at Urbana-Champaign.

### 2.2. Cognitive control paradigm

The cognitive task combined a flanker task and Go/NoGo task, but only the flanker task is discussed herein, given near ceiling performance on NoGo trials for all children ( $M = 98.2\%$ ,  $SD = 2.8\%$ ) and our hypotheses about attentional and interference control. Five shapes were presented on an MRI back projection, and participants were instructed to look at the middle shape. Here, we analyze neutral ( $\rightarrow\rightarrow\rightarrow$ ,  $\leftarrow\leftarrow\leftarrow$ ) and incongruent ( $\leftarrow\leftarrow\leftarrow\leftarrow$ ,  $\rightarrow\rightarrow\rightarrow\rightarrow$ ) trials. When the middle arrow pointed to the left, participants were instructed to press a button with their left index finger. When the middle arrow pointed to the right, participants were instructed to press a button with their right index finger. The incongruent condition required additional attention and interference control to filter potentially misleading flankers that were mapped to incorrect behavioral responses. The neutral task condition was designed to act as a baseline comparison for the incongruent (and NoGo) trials. Piloting the task and Bunge, Dudukovic, Thomason, Vaidya, and Gabrieli (2002) suggest that congruent flanker trials ( $\rightarrow\rightarrow\rightarrow\rightarrow$ ,  $\leftarrow\leftarrow\leftarrow\leftarrow$ ) and neutral trials ( $\rightarrow\rightarrow\rightarrow$ ,  $\leftarrow\leftarrow\leftarrow$ ) yield similar performance.

During the task, 20 trials of each of the neutral and incongruent shape presentations ( $\rightarrow\rightarrow\rightarrow$ ,  $\leftarrow\leftarrow\leftarrow$ ,  $\rightarrow\rightarrow\leftarrow$ ,  $\leftarrow\leftarrow\rightarrow$ ) were presented in a random order, yielding a total of 80 trials. The response window included the presentation of the array of shapes for 500 ms, followed by a blank screen for 1000 ms. Each stimulus array was separated by a fixation cross (+) presented for 1500 ms. Additional fixation crosses that jittered between 1500 ms and 6000 ms were also randomly presented after the constant 1500 ms fixation cross throughout the task to prevent participants from expecting a specific frequency of responding. White shapes and white fixation crosses were presented on a black background. The participant was engaged in the

task for about 6 min. Stimulus presentation, timing, and task performance measures were controlled by E-Prime software.

### 2.3. Magnetic resonance imaging acquisition

Diffusion-weighted images were acquired on a Siemens Magnetom Trio 3T whole-body scanner with repetition time (TR)=4400 ms, echo time (TE)=98 ms and 1.72 mm<sup>2</sup> in-plane resolution with 3 mm slice thickness. To obtain whole-head coverage, 32 slices were collected parallel to the anterior–posterior commissure plane with no interslice gap. Four T2-weighted images ( $b$ -value=0 s/mm<sup>2</sup>) and two repetitions of 30-direction diffusion-weighted echo planar imaging scans ( $b$ -value=1000 s/mm<sup>2</sup>) were collected.

Diffusion information can be represented mathematically as a diffusion tensor/diffusion ellipsoid. FA is calculated from the three eigenvalues ( $\lambda_1, \lambda_2, \lambda_3$ ) of the diffusion tensor and represents anisotropic (directionally dependent) diffusion (Basser, 1995; Beaulieu, 2002; Sen & Basser, 2005), independently of the rate of diffusion. FA ranges from 0 to 1, with higher values reflecting increased directionality of diffusion (i.e., water traveling more parallel to a tract compared to perpendicularly). In a region with free diffusion, the FA value is 0 and the diffusion is isotropic. If the diffusion is more in one direction, i.e., anisotropic diffusion, the FA value approaches 1. MD represents the mean of all three axes of the diffusion ellipsoid ( $(\lambda_1 + \lambda_2 + \lambda_3)/3$ ), which is the average rate of water diffusion, independent of direction. AD is the diffusion along the principal diffusion eigenvalue ( $\lambda_1$ ) of the ellipsoid. RD is the average of the second and third eigenvalues ( $\lambda_2, \lambda_3$ ), reflective of diffusivity perpendicular to the major axis of the tensor (Basser, 1995; Pierpaoli & Basser, 1996; Pierpaoli et al., 1996; Song et al., 2002).

### 2.4. Diffusion data analysis

Image analyses and tensor calculations were performed using FSL 4.1.9 (FMRIB Software Library). First, each participant's data were passed through an automated pipeline consisting of (1) motion and eddy current correction, (2) removal of non-brain tissue using the Brain Extraction Tool (Smith, 2002), and (3) local fitting of the diffusion tensor model at each voxel using FMRIB's Diffusion Toolbox v2.0 (FDT: <http://www.fmrib.ox.ac.uk/fsl/fdt>). The products of the multi-step pipeline included FA, MD and AD images; RD maps were calculated as the mean of the second and third eigenvalues (Song et al., 2002).

Next, diffusion data were processed using TBSS v1.2 (Tract-Based Spatial Statistics, Smith et al., 2006). Each participant's FA data were aligned into the 1 mm × 1 mm × 1 mm standard Montreal Neurological Institute (MNI152) space via the FMRIB58\_FA template using the FMRIB's Nonlinear Registration Tool (Andersson, Jenkinson, & Smith, 2007a, 2007b), and a mean diffusion image was created. The mean FA image was then thinned to create an average skeleton representing the centers of the tracts shared by all participants, and the skeleton was thresholded at FA > 0.20. Each participant's aligned FA data were projected onto the skeleton, taking on the FA value from the local center of the nearest relevant tract. MD, AD, and RD skeletons for each participant were formed in a similar manner by projecting the analogous data onto the mean skeleton.

### 2.5. Region-of-interest analysis

Diffusion values (FA, MD, AD, RD) were calculated for each participant *a priori* ROIs, created from the JHU ICBM-DTI-81 white matter labels atlas (<http://www.fmrib.ox.ac.uk/fsl/data/atlas-descriptions.html#wm> [Hua et al., 2008; Mori, Wakana, & Van Zijl, 2005; Wakana et al., 2007]). Tract ROIs were created in the left and right corpus callosum, corona radiata, superior longitudinal fasciculus, posterior thalamic radiation, and cerebral peduncle (Fig. 1). An FSL command, `fslmaths`, was used to create each ROI (e.g., `fslmaths JHUAtlas -uthr 16 -thr 16 RCerebralPeduncle`). Because DTI measures in left and right lateralized tracts were highly correlated (all  $r > 0.5$ , all  $p < 0.0001$ ), an average diffusion value across left and right hemispheres was computed for each ROI for each diffusion measure for each participant.

### 2.6. Statistical analyses

Repeated measures ANOVAs were conducted to examine differences in task performance (RT, accuracy) during incongruent and neutral trials. A MANOVA was conducted to examine the omnibus relationship between DTI measures and task performance. Then, given the *a priori* hypotheses, partial correlations were conducted to examine the relationship between mean task performance and white matter microstructure, as measured with FA, MD, AD, and RD, while controlling for age. Interference cost scores were calculated to investigate how white matter microstructure was associated with the amount of behavioral interference engendered by incongruent flanking items relative to neutral trials. An interference score was computed for each participant as [(neutral performance – incongruent performance)/neutral performance] × 100%. The interference cost score helps quantify the amount of cost associated with the response incompatible flanker arrows during the incongruent task condition compared to the neutral task condition. Task performance and DTI measures across the 61 child participants are provided in Table 1.

## 3. Results

### 3.1. Task performance

Children showed shorter RT ( $F(1, 60)=81.566, p < 0.001$ ) for neutral trials ( $M=857.397$  ms,  $SE=16.888$  ms) compared to incongruent trials ( $M=935.829$  ms,  $SE=18.587$  ms), as well as higher accuracy ( $F(1, 60)=51.648, p < 0.001$ ) during neutral trials ( $M=87.100\%$ ,  $SE=1.400\%$ ) compared to incongruent trials ( $M=78.900\%$ ,  $SE=2.000\%$ ).

### 3.2. Diffusion tensor imaging and task performance

MANOVAs with all bilateral FA, MD, AD, and RD values as the dependent measures and task performance as individual fixed factors yielded marginal, yet non-significant, results (i.e., Wilks'  $\lambda$ ; all  $F < 1.300, p > 0.060$ ). Since we approached our study with *a priori* hypotheses, we conducted several post hoc analyses to test correlations between performance and diffusion FA values from ROIs, while controlling for age (given that age correlated with incongruent accuracy [ $r=0.267, p=0.04$ ]). See Table 2 for correlation matrix.

Here we summarize the correlations that reached significance. Incongruent accuracy was positively correlated with FA in the corona radiata ( $r=0.283, p=0.029$ ), posterior thalamic radiation ( $r=0.359, p=0.005$ ), and cerebral peduncle ( $r=0.259, p=0.046$ ). These correlations suggest that superior attentional and interference control is associated with higher estimates of white matter integrity in specific tracts, independent of age. In addition, incongruent accuracy was negatively correlated with MD in the posterior thalamic radiation ( $r=-0.305, p=0.018$ ) as well as RD in the corona radiata ( $r=-0.265, p=0.041$ ) and posterior thalamic radiation ( $r=-0.346, p=0.007$ ), which suggests that improved performance is associated with higher estimates of membrane density and myelination in some white matter tracts.

Neutral accuracy was negatively correlated with FA in the posterior thalamic radiation ( $r=0.266, p=0.04$ ), MD in the posterior thalamic radiation ( $r=-0.275, p=0.033$ ), AD in the superior longitudinal fasciculus ( $r=-0.264, p=0.041$ ), and RD in the posterior thalamic radiation ( $r=-0.278, p=0.032$ ), which suggests that superior attentional allocation may relate to higher estimates of membrane density, axonal diameter, and myelination in some white matter tracts. No significant associations between white matter microstructure and incongruent RT, neutral RT, or interference cost (RT) reached significance.

Interference cost scores, in terms of accuracy, were correlated with FA in the cerebral peduncle ( $r=-0.328, p=0.01$ ), FA in the posterior thalamic radiation ( $r=-0.327, p=0.01$ ) as well as RD in the cerebral peduncle ( $r=0.291, p=0.024$ ), when controlling for age. These associations suggest that less interference is associated with greater estimates of white matter microstructure in specific white matter tracts. The correlations provide additional support for the importance of these tracts in incongruent and neutral task accuracy noted in the correlations reported above.

## 4. Discussion

The present investigation used DTI to explore the extent to which white matter microstructure is related to cognitive control in 7–9-year-old children. Cognitive control is said to be supported by a network of frontal, parietal, striatal and motor regions (Banich et al., 2000), and the present study examined tracts that travel throughout these brain regions to try to locate the specific white matter fibers important for attentional and interference control. Our results suggest that 7–9-year-old children with better estimates of white matter integrity in terms of

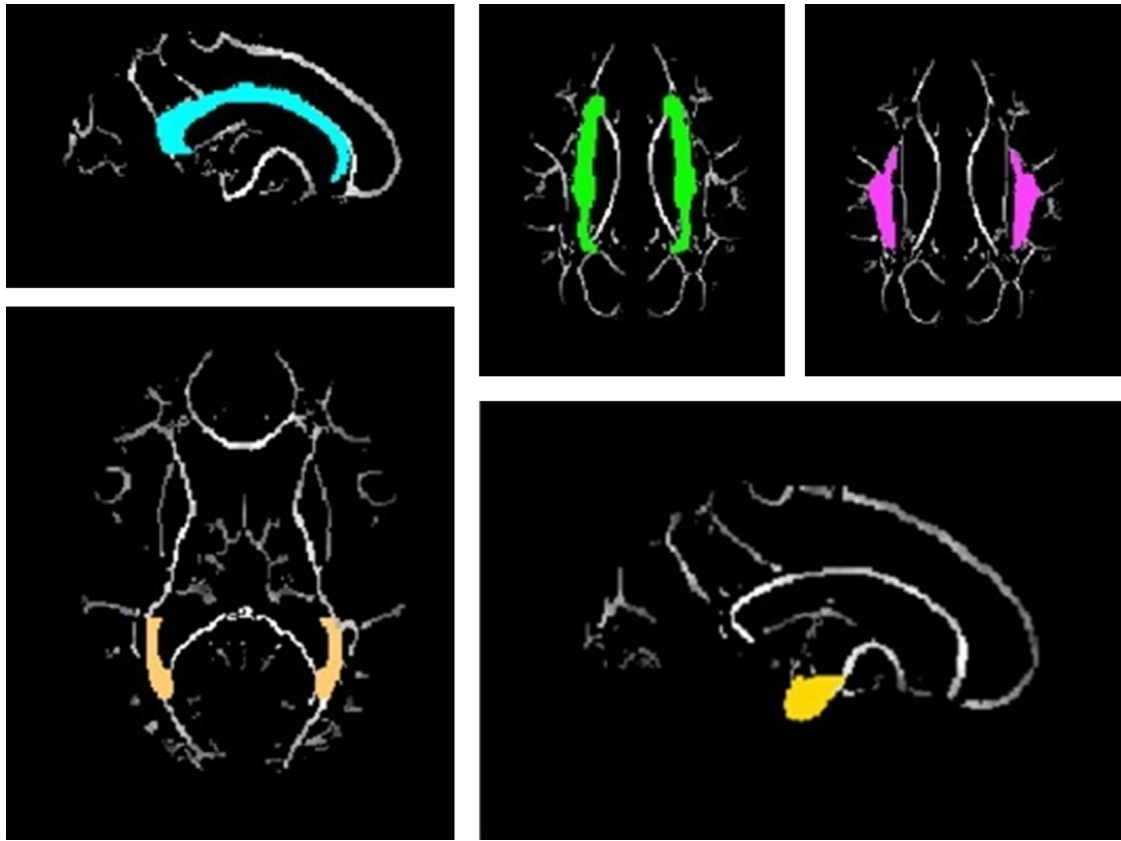


**Fig. 1.** Illustrations of the white matter tract ROIs. Corpus callosum (blue), corona radiata (green), superior longitudinal fasciculus (purple), posterior thalamic radiation (beige), and cerebral peduncle (yellow).

FA, MD, AD, and RD, in portions of the corona radiata, superior longitudinal fasciculus, posterior thalamic radiation, and cerebral peduncle, are more accurate on overall trials during a task measuring cognitive control, selective attention, and interference suppression. Importantly, the data suggest that higher estimates

of microstructure in the posterior thalamic radiation and cerebral peduncle are associated with a child's ability to suppress interfering information and exhibit increased attentional control (i.e., interference cost score, incongruent and neutral difference scores).

**Table 1**

Mean, standard deviation (SD), and range of task performance and DTI measures across 61 children.

|  | Mean       | SD       | Range             |
|--|------------|----------|-------------------|
| Incongruent RT (ms)                    | 940.304    | 142.683  | 668.14–1260.25    |
| Neutral RT (ms)                        | 864.294    | 127.755  | 648.86–1162.43    |
| Incongruent accuracy (percent correct) | 78.85      | 1.53     | 38.00–100.00      |
| Neutral accuracy (percent correct)     | 87.13      | 1.060    | 55.00–100.00      |
| Interference cost (RT)                 | 9.4411     | 8.3706   | –7.49–38.70       |
| Interference cost (accuracy)           | 9.9178     | 11.0311  | –8.09–46.67       |
| FA corpus callosum                     | 0.6933     | 0.02456  | 0.62–0.74         |
| FA corona radiata                      | 0.4770     | 0.02085  | 0.43–0.51         |
| FA superior longitudinal fasciculus    | 0.4784     | 0.02309  | 0.42–0.52         |
| FA posterior thalamic radiation        | 0.6055     | 0.02911  | 0.53–0.68         |
| FA cerebral peduncle                   | 0.6675     | 0.02621  | 0.58–0.72         |
| MD corpus callosum                     | 0.00079496 | 0.000029 | 0.000737–0.000895 |
| MD corona radiata                      | 0.00077920 | 0.000026 | 0.000723–0.000866 |
| MD superior longitudinal fasciculus    | 0.00073307 | 0.000026 | 0.000668–0.000827 |
| MD posterior thalamic radiation        | 0.00083811 | 0.000031 | 0.000770–0.000958 |
| MD cerebral peduncle                   | 0.00075922 | 0.000027 | 0.000722–0.000871 |
| AD corpus callosum                     | 0.00156877 | 0.000037 | 0.001481–0.001653 |
| AD corona radiata                      | 0.00122521 | 0.000034 | 0.001161–0.001315 |
| AD superior longitudinal fasciculus    | 0.00113493 | 0.00003  | 0.001069–0.001217 |
| AD posterior thalamic radiation        | 0.00150504 | 0.000041 | 0.001402–0.001600 |
| AD cerebral peduncle                   | 0.00145700 | 0.000039 | 0.001362–0.001552 |
| RD corpus callosum                     | 0.00040802 | 0.000035 | 0.000349–0.000532 |
| RD corona radiata                      | 0.00055623 | 0.000029 | 0.000502–0.000641 |
| RD superior longitudinal fasciculus    | 0.00053212 | 0.00003  | 0.000467–0.000632 |
| RD posterior thalamic radiation        | 0.00050460 | 0.000038 | 0.000438–0.000645 |
| RD cerebral peduncle                   | 0.00041033 | 0.00003  | 0.000358–0.000535 |

**Table 2**

Correlations between white matter microstructure and performance on a cognitive control task (including age as a covariate). No associations between white matter structure and incongruent RT and neutral RT reached significance.

|                                     | Incongruent accuracy  | Neutral accuracy     | Interference cost (accuracy) |
|-------------------------------------|-----------------------|----------------------|------------------------------|
| FA corpus callosum                  | 0.103 ( $p=0.4$ )     | 0.108 ( $p=0.4$ )    | -0.168 ( $p=0.2$ )           |
| FA corona radiata                   | 0.283* ( $p=0.03$ )   | 0.234 ( $p=0.07$ )   | -0.162 ( $p=0.2$ )           |
| FA superior longitudinal fasciculus | 0.065 ( $p=0.6$ )     | -0.055 ( $p=0.7$ )   | -0.114 ( $p=0.4$ )           |
| FA posterior thalamic radiation     | 0.359* ( $p=0.005$ )  | 0.266* ( $p=0.04$ )  | -0.324* ( $p=0.01$ )         |
| FA cerebral peduncle                | 0.259* ( $p=0.05$ )   | 0.08 ( $p=0.5$ )     | -0.283* ( $p=0.03$ )         |
| MD corpus callosum                  | -0.081 ( $p=0.5$ )    | -0.014 ( $p=0.9$ )   | 0.093 ( $p=0.5$ )            |
| MD corona radiata                   | -0.206 ( $p=0.1$ )    | -0.187 ( $p=0.2$ )   | 0.146 ( $p=0.3$ )            |
| MD superior longitudinal fasciculus | -0.171 ( $p=0.2$ )    | -0.116 ( $p=0.4$ )   | 0.144 ( $p=0.3$ )            |
| MD posterior thalamic radiation     | -0.305* ( $p=0.02$ )  | -0.275* ( $p=0.03$ ) | 0.195 ( $p=0.1$ )            |
| MD cerebral peduncle                | -0.09 ( $p=0.5$ )     | 0.03 ( $p=0.8$ )     | 0.109 ( $p=0.4$ )            |
| AD corpus callosum                  | -0.005 ( $p=0.9$ )    | 0.16 ( $p=0.2$ )     | 0.010 ( $p=0.9$ )            |
| AD corona radiata                   | -0.036 ( $p=0.8$ )    | -0.06 ( $p=0.6$ )    | 0.116 ( $p=0.4$ )            |
| AD superior longitudinal fasciculus | -0.207 ( $p=0.1$ )    | -0.264* ( $p=0.04$ ) | 0.064 ( $p=0.6$ )            |
| AD posterior thalamic radiation     | -0.033 ( $p=0.8$ )    | -0.094 ( $p=0.5$ )   | -0.115 ( $p=0.4$ )           |
| AD cerebral peduncle                | 0.191 ( $p=0.1$ )     | 0.16 ( $p=0.2$ )     | -0.164 ( $p=0.2$ )           |
| RD corpus callosum                  | -0.095 ( $p=0.5$ )    | -0.014 ( $p=0.9$ )   | 0.109 ( $p=0.4$ )            |
| RD corona radiata                   | -0.265 ( $p=0.07$ )   | -0.221 ( $p=0.09$ )  | 0.177 ( $p=0.2$ )            |
| RD superior longitudinal fasciculus | -0.118 ( $p=0.37$ )   | -0.018 ( $p=0.9$ )   | 0.122 ( $p=0.4$ )            |
| RD posterior thalamic radiation     | -0.346* ( $p=0.007$ ) | -0.278* ( $p=0.03$ ) | 0.256* ( $p=0.04$ )          |
| RD cerebral peduncle                | -0.231 ( $p=0.075$ )  | -0.075 ( $p=0.6$ )   | 0.177 ( $p=0.2$ )            |

\*  $p < 0.05$ .

This study supports and extends previous research on the association between the structure of specific white matter tracts and cognition (see Table 2 in Madden et al., 2012 for review of the associations between white matter structure and cognition across the lifespan). The corona radiata has ascending and descending tracts from the cerebral cortex that integrate information throughout the brain, and these tracts are known to play a role in processing speed, cognitive control and memory (Bendlin et al., 2010; Niogi et al., 2010; Olesen et al., 2003). The superior longitudinal fasciculus provides bidirectional information transfer between the frontal and parietal cortex (Petrides & Pandya, 1984; Schmahmann & Pandya, 2006), and these connections have been found to correlate with performance on a task of working memory in children (Nagy et al., 2004) as well as in older adults (Burzynska et al., 2011). We extend the cognitive associations of these tracts to include attentional control (i.e., performance on incongruent and neutral trials that require varying amounts of cognitive control). Furthermore, we suggest that the posterior thalamic radiation, which includes axons connecting the cerebral cortex, basal ganglia, and thalamus, and the cerebral peduncle, which are fibers that convey motor information to and from the brain to the rest of the body, also play a role in overall cognitive control and interference control. Together, we speculate that the white matter microstructure of a circuit of frontal, parietal, striatal, and motor regions is associated with performance on a task of selective attention, inhibition of distractions, and maintenance of information in working memory.

By analyzing a number of parameters of the diffusion ellipsoid, each reflective of distinct aspects of white matter microstructure, we contribute to the understanding of mechanisms involved in cognitive control in children. It seems that better control abilities in 7–9-year-old children relate to higher FA values in the corona radiata, posterior thalamic radiation, and cerebral peduncle, particularly when increased attentional control and interference control are required, which suggests that these compact tracts with uniform fiber alignment are important for increased cognitive control. Greater integrity in these regions may originate from a reduction in RD, which could suggest more myelinated axons (Song et al., 2003; Song et al., 2005; Sun et al., 2006; Sun, Liang, Cross, & Song, 2008). Estimates of membrane density of axons, particularly in the posterior thalamic radiation, as well as axonal diameter, particularly in the superior longitudinal fasciculus, may also play a role in a child's ability to pay attention during high and low cognitive

demands. Because both axonal caliber and thickness of the myelin sheath determine conduction velocity (Paus, 2010), the results raise the possibility that children with higher task performance may have faster neural conduction between brain regions involved in attention and motor control.

These results have implications for development. Structural brain changes during childhood likely reflect an interplay among changes in cell proliferation and apoptosis, dendritic branching and pruning, and synaptic formation and elimination, in accord with the strengthening of relevant neural connections and the pruning of inefficient pathways (Andersen, 2003). Intra-cortical myelination is also said to play a role in development (Paus, 2005). White matter, including tracts that connect frontal, parietal, motor and striatal regions, has been found to increase roughly linearly throughout childhood (e.g., Barnea-Goraly et al., 2005; Bonekamp et al., 2007; Lebel & Beaulieu, 2011; Schmithorst, Wilke, Dardzinski, & Holland, 2002; Schmithorst & Yuan, 2010). Here, we provide cognitive significance for these changes by suggesting that improved structure in developing tracts such as the corona radiata (Keller et al., 2007), longitudinal fasciculus (Bonekamp et al., 2007), and motor regions (Barnea-Goraly et al., 2005) is associated with superior cognition. The inclusion of overall scores on the cognitive control task as well as interference cost scores help provide insight into the tracts important for performance on challenges of varying difficulty.

The present study's correlations between white matter fibers and flanker task accuracy extend Tamnes et al.'s (2012) observations of associations between white matter microstructure and flanker RT performance variability. Whereas Tamnes et al. (2012) reported correlations between intraindividual variability for congruent and incongruent flanker trials and white matter microstructure in the corpus callosum, left superior longitudinal fasciculus, corticospinal tract, uncinate fasciculus, and forceps minor, we report relationships between incongruent and neutral accuracy (and their difference scores) and white matter integrity in the corona radiata, superior longitudinal fasciculus, posterior thalamic radiation, and cerebral peduncle. We did not find that flanker accuracy related to estimates of white matter microstructure of the corpus callosum, a tract that plays a role in information transfer. We speculate that differences in the age group of our samples, different flanker task designs (e.g., horizontal arrows versus vertical arrows, congruent versus neutral task condition), or different associations between percent correct and speed of responding

and white matter microstructure may explain the complementary yet disparate results. Neither study found associations between estimates of white matter architecture and mean RT. Both studies add to the role of white matter tracts in flanker task performance, but future research is needed to help dissociate the specific performance measures of attention and interference suppression that relate to specific white matter microstructure. Together these studies suggest that a circuit of cognitive and motor white matter fibers is important for cognitive control in children.

This study provides a first step in identifying the relationship between white matter microstructure and cognitive control. Because we approached the study with *a priori* hypotheses, additional investigations should employ whole-brain analyses corrected for multiple comparisons as well as explore the role of gender. In addition, it is important to remember that DTI does not measure tissue parameters (e.g., fiber integrity, myelination) directly, but measures the displacement of water molecules. Thus, indices of underlying microstructural properties can only be estimated from this displacement. Furthermore, the neutral condition of our modified flanker task is less well-known and requires additional exploration (but see Bunge et al., 2002). Despite these limitations, we demonstrate a circuit of white matter tracts important for cognitive control in 7–9-year-old children. The study contributes to the literature on the relationship between the developing brain and cognitive abilities important for learning and scholastic achievement during childhood.

## Acknowledgments

Thank you to Holly Tracy and Nancy Dodge for their help with data collection. This work was supported by a grant (HD055352) from the National Institute of Child Health and Human Development to Dr. Charles Hillman.

## References

- Andersen, S. L. (2003). Trajectories of brain development: Point of vulnerability or window of opportunity? *Neuroscience and Biobehavioral Reviews*, 27, 3–18.
- Andersson, J. R., Jenkinson, M., & Smith, S. (2007a). *TR07JA1: Non-linear optimisation*. Retrieved from [www.fmrib.ox.ac.uk/analysis/techrep](http://www.fmrib.ox.ac.uk/analysis/techrep)
- Andersson, J. R., Jenkinson, M., & Smith, S. (2007b). *TR07JA2: Non-linear registration, aka spatial normalisation*. Retrieved from [www.fmrib.ox.ac.uk/analysis/techrep](http://www.fmrib.ox.ac.uk/analysis/techrep)
- Banich, M. T., Milham, M. P., Atchley, R. A., Cohen, N. J., Webb, A., Wszalek, T., et al. (2000). fMRI studies of Stroop tasks reveal unique roles of anterior and posterior brain systems in attentional selection. *Journal of Cognitive Neuroscience*, 12, 988–1000.
- Barnea-Goraly, N., Menon, V., Eckert, M., Tamm, L., Bammer, R., Karchemskiy, A., et al. (2005). White matter development during childhood and adolescence: A cross-sectional diffusion tensor imaging study. *Cerebral Cortex*, 15, 1848–1854.
- Basser, P. J. (1995). Inferring microstructural features and the physiological state of tissues from diffusion-weighted images. *NMR in Biomedicine*, 8, 333–344.
- Beaulieu, C. (2002). The basis of anisotropic water diffusion in the nervous system: A technical review. *NMR in Biomedicine*, 15, 435–455.
- Bendlin, B. B., Fitzgerald, M. E., Ries, M. L., Xul, G., Kastman, E. K., Thiel, B. W., et al. (2010). White matter in aging and cognition: A cross-sectional study of microstructure in adults aged eighteen to eighty-three. *Developmental Neuropsychology*, 35, 257–277.
- Bonekamp, D., Nagae, L. M., Degaonkar, M., Matson, M., Abdalla, W. M., Barker, P. B., et al. (2007). Diffusion tensor imaging in children and adolescents: Reproducibility, hemispheric, and age-related differences. *NeuroImage*, 34, 733–742.
- Budde, M. D., Kim, J. H., Liang, H. F., Schmidt, R. E., Russell, J. H., Cross, A. H., et al. (2007). Toward accurate diagnosis of white matter pathology using diffusion tensor imaging. *Magnetic Resonance in Medicine*, 57, 688–695.
- Bull, R., & Scerif, G. (2001). Executive functioning as a predictor of children's mathematics ability: Inhibition, switching, and working memory. *Developmental Neuropsychology*, 19, 273–293.
- Bunge, S. A., & Crone, E. A. (2009). Neural correlates of the development of cognitive control. In J. Rumsey, & M. Ernst (Eds.), *Neuroimaging in developmental clinical neuroscience* (pp. 22–37). Cambridge, UK: Cambridge University Press.
- Bunge, S. A., Dudukovic, N. M., Thomason, M. E., Vaidya, C. J., & Gabrieli, J. D. E. (2002). Immature frontal lobe contributions to cognitive control in children: Evidence from fMRI. *Neuron*, 33, 301–311.
- Burzynska, A. Z., Nagel, I. E., Preuschhof, C., Li, S. C., Lindenberg, U., Backman, L., et al. (2011). Microstructure of frontoparietal connections predicts cortical responsiveness and working memory performance. *Cerebral Cortex*, 21, 2261–2271.
- Davidson, M. C., Amso, D., Anderson, L. C., & Diamond, A. (2006). Development of cognitive control and executive functions from 4 to 13 years: Evidence from manipulations of memory, inhibition, and task switching. *Neuropsychologia*, 44, 2037–2078.
- DeStefano, D., & LeFevre, J. A. (2004). The role of working memory in mental arithmetic. *European Journal of Cognitive Psychology*, 16, 353–386.
- DuPaul, G. J., Power, T. J., Anastopoulos, A., & Reid, R. (1998). *ADHD rating scale – IV: Checklists, norms, and clinical interpretation*. New York, NY: Guilford Press.
- Hua, K., Zhang, J., Wakana, S., Jiang, H., Li, X., Reich, D. S., et al. (2008). Tract probability maps in stereotaxic spaces: Analyses of white matter anatomy and tract-specific quantification. *NeuroImage*, 39, 336–347.
- Johansen-Berg, H., & Behrens, T. E. (2009). *Diffusion MRI: From quantitative measurement to in vivo neuroanatomy*. San Diego, CA: Elsevier.
- Jones, D. K. (2011). *Diffusion MRI: Theory, methods, and applications*. New York: Oxford University Press.
- Kaufman, A. S., & Kaufman, N. L. (1990). *Kaufman Brief Intelligence Test*. Circle Pines, MN: AGS.
- Keller, T. A., Rajesh, K., & Just, M. A. (2007). A developmental study of the structural integrity of white matter in autism. *NeuroReport*, 18, 23–27.
- Lebel, C., & Beaulieu, C. (2011). Longitudinal development of human brain wiring continues from childhood into adulthood. *Journal of Neuroscience*, 31, 10937–10947.
- Liston, C., Watts, R., Tottenham, N., Davidson, M. C., Niogi, S., Ulug, A. M., et al. (2006). Fronto-striatal microstructure modulates efficient recruitment of cognitive control. *Cerebral Cortex*, 16, 553–560.
- Madden, D. J., Bennett, I. J., Burzynska, A., Potter, G. G., Chen, N., & Song, A. W. (2012). Diffusion tensor imaging of cerebral white matter integrity in cognitive aging. *Biochimica et Biophysica Acta*, 1822, 386–400.
- Madsen, K. S., Baaré, W. F., Vestergaard, M., Skimminge, A., Ejersbo, L. R., Ramsøy, T. Z., et al. (2010). Response inhibition is associated with white matter microstructure in children. *Neuropsychologia*, 48, 854–862.
- Mori, S. (2007). *Introduction to diffusion tensor imaging*. Amsterdam: Elsevier.
- Mori, S., Wakana, S., & Van Zijl, P. C. M. (2005). *MRI atlas of human white matter*. Amsterdam: Elsevier.
- Nagy, Z., Westerberg, H., & Klingberg, T. (2004). Maturation of white matter is associated with the development of cognitive functions during childhood. *Journal of Cognitive Neuroscience*, 16, 1227–1233.
- Nair, G., Tanahashi, Y., Low, H. P., Billings-Gagliardi, S., Schwartz, W. J., & Duong, T. Q. (2005). Myelination and long diffusion times alter diffusion-tensor-imaging contrast in myelin-deficient shiverer mice. *NeuroImage*, 28, 165–174.
- Niogi, S., Mukherjee, P., Ghajar, J., & McCandliss, B. D. (2010). Individual differences in distinct components of attention are linked to anatomical variations in distinct white matter tracts. *Frontiers in Neuroanatomy*, 4, 1–12.
- Oldfield, R. C. (1971). The assessment and analysis of handedness: The Edinburgh inventory. *Neuropsychologia*, 9, 97–113.
- Olesen, P., Nagy, Z., Westerberg, H., & Klingberg, T. (2003). Combined analysis of DTI and fMRI data reveals a joint maturation of white and grey matter in a fronto-parietal network. *Cognitive Brain Research*, 18, 48–57.
- Paus, T. (2005). Mapping brain maturation and cognitive development during adolescence. *Trends in Cognitive Sciences*, 9, 60–68.
- Paus, T. (2010). Growth of white matter in the adolescent brain: Myelin or axon? *Brain and Cognition*, 72, 26–35.
- Petrides, M., & Pandya, D. N. (1984). Projections to the frontal cortex from the posterior parietal region in the rhesus monkey. *Journal of Comparative Neurology*, 228, 105–116.
- Pierpaoli, C., & Basser, P. J. (1996). Toward a quantitative assessment of diffusion anisotropy. *Magnetic Resonance in Medicine*, 36, 893–906.
- Pierpaoli, C., Jezzard, P., Basser, P. J., Barnett, A., & Di Chiro, G. (1996). Diffusion tensor MR imaging of the human brain. *Radiology*, 201, 637–648.
- Rykhlevskaia, E., Gratton, G., & Fabiani, M. (2008). Combining structural and functional neuroimaging data for studying brain connectivity: A review. *Psychophysiology*, 45, 173–187.
- Schmahmann, J. D., & Pandya, D. N. (2006). *Fiber pathways of the brain*. New York: Oxford University Press.
- Schmithorst, V. J., Wilke, M., Dardzinski, B. J., & Holland, S. K. (2002). Correlation of white matter diffusivity and anisotropy with age during childhood and adolescence: A cross-sectional diffusion-tensor MR imaging study. *Radiology*, 222, 212–218.
- Schmithorst, V. J., & Yuan, W. (2010). White matter development during adolescence as shown by diffusion MRI. *Brain and Cognition*, 72, 16–25.
- Sen, P. N., & Basser, P. J. (2005). A model for diffusion in white matter in the brain. *Biophysical Journal*, 89, 2927–2938.
- Shaw, P., Greenstein, D., Lerch, J., Clasen, L., Lenroot, R., Gogtay, N., et al. (2006). Intellectual ability and cortical development in children and adolescents. *Nature*, 440, 676–679.
- Smith, S. M. (2002). Fast robust automated brain extraction. *Human Brain Mapping*, 17, 143–155.
- Smith, S. M., Jenkinson, M., Johansen-Berg, H., Rueckert, D., Nichols, T. E., Mackay, C., et al. (2006). Tract-based spatial statistics: Voxelwise analysis of multi-subject diffusion data. *NeuroImage*, 31, 1487–1505.
- Song, S. K., Sun, S. W., Ju, W. K., Lin, S. J., Cross, A. H., & Neufeld, A. H. (2003). Diffusion tensor imaging detects and differentiates axon and myelin degeneration in mouse optic nerve after retinal ischemia. *NeuroImage*, 20, 1714–1722.
- Song, S. K., Sun, S. W., Ramsbottom, M. J., Chang, C., Russell, J., & Cross, A. H. (2002). Dysmyelination revealed through MRI as increased radial (but unchanged axial) diffusion of water. *NeuroImage*, 17, 1429–1436.

- Song, S. K., Yoshino, J., Le, T. Q., Lin, S. J., Sun, S. W., Cross, A. H., et al. (2005). Demyelination increases radial diffusivity in corpus callosum of mouse brain. *NeuroImage*, *26*, 132–140.
- St. Clair-Thompson, H. L., & Gathercole, S. E. (2006). Executive functions and achievements in school: Shifting, updating, inhibition, and working memory. *The Quarterly Journal of Experimental Psychology*, *59*, 745–759.
- Sun, S. W., Liang, H. F., Cross, A. H., & Song, S. K. (2008). Evolving Wallerian degeneration after transient retinal ischemia in mice characterized by diffusion tensor imaging. *NeuroImage*, *40*, 1–10.
- Sun, S. W., Liang, H. F., Le, T. Q., Armstrong, R. C., Cross, A. H., & Song, S. K. (2006). Differential sensitivity of in vivo and ex vivo diffusion tensor imaging to evolving optic nerve injury in mice with retinal ischemia. *NeuroImage*, *32*, 1195–1204.
- Tamnes, C. K., Fjell, A. M., Westlye, L. T., Ostby, Y., & Walhovd, K. B. (2012). Becoming consistent: Developmental reductions in intraindividual variability in reaction time are related to white matter integrity. *Journal of Neuroscience*, *32*, pp 972–892.
- Taylor, S. J. C., Whincup, P. H., Hindmarsh, P. C., Lampe, F., Odoki, K., & Cook, D. G. (2001). Performance of a new pubertal self-assessment questionnaire: A preliminary study. *Paediatric and Perinatal Epidemiology*, *15*, 88–94.
- Wakana, S., Caprihan, A., Panzenboeck, M. M., Fallon, J. H., Perry, M., Gollub, R. L., et al. (2007). Reproducibility of quantitative tractography methods applied to cerebral white matter. *NeuroImage*, *36*, 630–644.